



## Whole mantle discontinuity structure beneath Hawaii

Anna M. Courtier,<sup>1</sup> Brian Bagley,<sup>1</sup> and Justin Revenaugh<sup>1</sup>

Received 15 June 2007; revised 23 July 2007; accepted 7 August 2007; published 11 September 2007.

[1] We examined mantle structure beneath the southeast Hawaiian Islands using multiple *ScS* reverberations from four earthquakes from the island of Hawaii and recorded at station KIP on the island of Oahu. We find an unusually deep 410-km discontinuity and a transition zone thickness of 227 km, corresponding to a temperature increase of 87 K above the global average. Other reflectors include a lid-low-velocity zone boundary, a weak 520-km discontinuity, and smaller discontinuities at 224 km, 288 km, and 1000 km. Whole mantle travel time is near the global average, which we attribute to an inclined or branching plume, lowermost mantle anisotropy, and estimate bias due to a possible ultra-low velocity zone atop the core. **Citation:** Courtier, A. M., B. Bagley, and J. Revenaugh (2007), Whole mantle discontinuity structure beneath Hawaii, *Geophys. Res. Lett.*, *34*, L17304, doi:10.1029/2007GL031006.

### 1. Introduction

[2] The theory that intraplate, volcanic oceanic islands result from deep-seated, thermal mantle plumes is the subject of intense scientific debate (for a review, see *Anderson* [2005]). Although seismic studies have imaged the structures as narrow regions with seismically slow velocities extending to great depth in the mantle [*Allen et al.*, 1999; *Montelli et al.*, 2004, 2006], others suggest that plumes originate in the upper mantle [*Anderson*, 2000] or that they are purely chemical anomalies [e.g., *Takahashi et al.*, 1998].

[3] The distance between the 410-km and 660-km seismic discontinuities can be used to indicate whether mantle plumes have thermal anomalies. The discontinuities mark phase transitions in the olivine component of the mantle: from olivine to wadsleyite at 410 km and the dissociation of ringwoodite to perovskite and ferro-periclase at 660 km (see *Helfrich* [2000] for a review). The pressure-temperature trajectories of these reactions are described by their Clapeyron slopes. The reaction corresponding to the 410-km discontinuity has a steeper Clapeyron slope (4.0 MPa/K) [*Katsura et al.*, 2004] than that of the 660-km discontinuity (−2.0 to −0.4 MPa/K) [*Katsura et al.*, 2003] and is opposite in sign. This results in the 410-km and the 660-km transitions deflecting towards each other in the presence of increased transition zone (TZ) temperature, with a stronger deflection at 410 km, assuming a through-going thermal anomaly.

[4] Global studies of TZ thickness (TZT) by *Flanagan and Shearer* [1998] and *Lawrence and Shearer* [2006] obtain a global average thickness of 241 and 242 km, respectively. Both studies observe thickening of the TZ

near subduction zones and average or thinned TZTs beneath ocean basins.

[5] Measurements of TZT cannot address whether a thermal anomaly originates in the deep upper mantle or at the core-mantle boundary. Combining the observations with mantle travel time measurements yields further information about the existence of mantle plumes and their structures. Lower seismic velocity is an expected effect of a thermal plume [*Sleep*, 2006], which should result in a delayed mantle travel time relative to global reference mantle models. Whole-mantle travel times are generally obtained through analysis of differential times between multiple *ScS* arrivals [e.g., *Okal and Anderson*, 1975; *Lay and Wallace*, 1983]. Individual measurements of *ScS* travel time ( $T_{ScS}$ ) average heterogeneity across the depth of the entire mantle and cannot differentiate between strong anomalies concentrated in one depth range in the mantle and weaker whole-mantle anomalies.

[6] Several studies have investigated the mantle beneath the Hawaiian Islands, a region that is characterized by slow velocities [e.g., *Megnin and Romanowicz*, 2000] and is commonly thought to be the result of a thermal whole-mantle plume, being in many respects the poster-child of deep mantle plumes. Petrologic studies have investigated the region [e.g., *Herzberg*, 2006], and the local TZ discontinuity structure has been examined seismically using *SS*-precursors [*Schmerr and Garnero*, 2006] and receiver functions [*Li et al.*, 2000; *Shen et al.*, 2003]. All three studies observe a thinned TZ beneath Hawaii, with thickness estimates ranging from ~200 to 230 km, consistent with the effects of a thermal plume. The region has also been examined with seismic tomography [*Montelli et al.*, 2004, 2006; *Lei and Zhao*, 2006] and differential analysis of multiple *ScS* phases [*Sipkin and Jordan*, 1980]. We utilize multiple *ScS* reverberations to estimate  $T_{ScS}$  and TZ discontinuity structure jointly beneath the region with the waveform inversion/migration method of *Revenaugh and Jordan* [1991a, 1991b]. Our estimates of  $T_{ScS}$  incorporate the effects of crustal structure and mantle attenuation on the multiple *ScS* waveforms. The sensitivity of *ScS* reverberations to absolute two-way travel time (not one-way differential time as is the case for receiver function methods) results in accurate discontinuity depth estimates despite the effects of local velocity anomalies.

### 2. Data and Method

[7] We examined all digital long-period and broadband records of magnitude  $\geq 5.7$  earthquakes located beneath the island of Hawaii and recorded along the island chain. Records were culled to eliminate those with excessively low signal-to-noise ratios. *ScS* is not commonly observed clearly for shallow-focus events, and our 35-year catalog of seismicity produced only four events with usable seismo-

<sup>1</sup>Department of Geology and Geophysics, University of Minnesota, Minneapolis, Minnesota, USA.

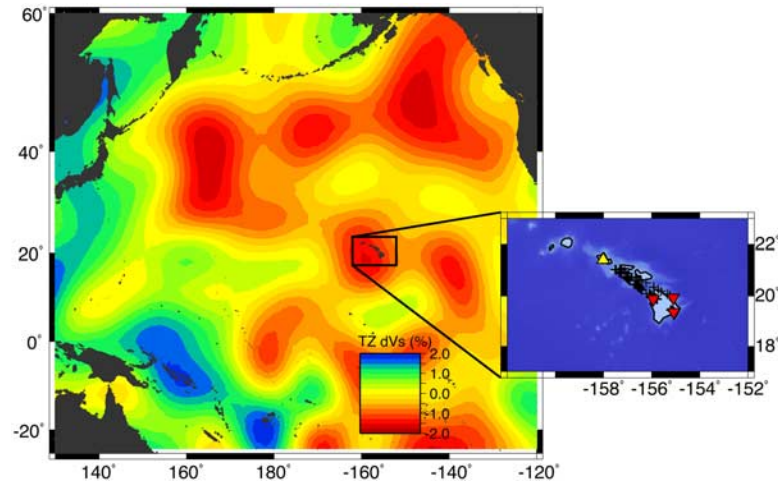


**Figure 1.** Regional map showing contours of vertically averaged velocity deviation within the TZ from the SH tomographic model SAW24B16 [Megnin and Romanowicz, 2000]. Inset: Map showing sources (red inverted triangles), receiver (yellow triangle), and multiple  $ScS$  surface bounce-point locations (crosses) across the study area.

grams, all recorded by station KIP on the island of Oahu (Figure 1 and Table 1). The source-receiver corridor has an epicentral distance of approximately  $3^\circ$ , resulting in near-vertical incidence for the multiple  $ScS$  reverberations. This allows us to use both the radial and transverse components to investigate SH-reflectivity in the mantle along the corridor. While noise (ambient or signal generated) is not independent between components, the use of both does afford some increase in noise suppression due to the variations in polarity between signal and non-signal generated noise. The only exception to this was the 1973 event, where only the east component was used due to natural east-west alignment of particle motion. Seismograms were deconvolved to ground velocity, decimated to a three-second sampling interval, and filtered with a cosine-squared band-pass filter between 8 and 60 mHz, with filter corners at 10 and 45 mHz (Figure S1).<sup>1</sup>

[8] We used the hierarchical waveform inversion and migration method of Revenaugh and Jordan [1991a, 1991b] to model both zeroth- and first-order  $ScS$  reverberations. Zeroth-order  $ScS$  reverberations are multiple  $ScS$  and  $sScS$  phases; first-order reverberations are similar but are reflected once from a mantle discontinuity along the path between the source and receiver (Figure S2). A minimum of two and maximum of four  $ScS_n$ - $sScS_n$  pairs ( $n = 1-4$ ) were modeled for each seismogram. Values for crustal thickness,  $T_{ScS}$ , and whole-mantle attenuation along the source-receiver path were obtained through waveform modeling of the zeroth-order reverberations. Synthetic zeroth-order reverberations were then stripped from the data, resulting in a residual signal dominated by first- and higher-order reverberations [Revenaugh and Jordan, 1989]. One-dimensional migration of the first-order reverberations [Revenaugh and Jordan, 1991b] yields a radial profile of SH-reflectivity in the mantle. Synthetic seismograms are migrated iteratively to produce a synthetic reflection profile closely matching the data profile. The discontinuity depths included in the synthetic profile were corrected for bathymetry, crustal thick-

ness, and background mantle heterogeneity (M84C) [Woodhouse and Dziewonski, 1984] following Revenaugh and Jordan [1991b] and are referenced to PREM [Dziewonski and Anderson, 1981].

### 3. Results

[9] We present discontinuity depths and impedance contrasts inferred beneath the study area (Table 2) and the corresponding data and synthetic reflectivity profiles (Figure 2). The first synthetic reflectivity profile includes only the Gutenberg (indicative of a low-velocity layer at  $\sim 100$  km), 410-, 520-, and 660-km discontinuities, and fits the data profile very closely. Additional discontinuities in the upper and mid-mantle were modeled in the second synthetic profile. The amplitudes of these reflectors do not exceed our 95% confidence limits but were included on the basis of other nearby observations [Deuss and Woodhouse, 2002; Shen et al., 2003]. While confidence in this model is lower, the profile does match the data very closely. There is no evidence for an additional low-velocity layer directly atop the TZ as has been suggested for some regions thought to be associated with mantle plumes [Vinnik et al., 2003]. The depths and impedance contrasts for discontinuities included in both synthetic profiles change slightly due to interactions from first- and higher-order reverberations from the additional discontinuities included in the second synthetic profile. We use the results from the first, more conservative, synthetic profile in the following discussion of TZT and the corresponding thermal anomalies.

[10] We incorporated crustal structure and whole-mantle attenuation into waveform modeling, yielding a vertical-

**Table 1.** Source Parameters for Events Used in the Study

Date	Lat	Lon	Depth, km	$mb$
April 26, 1973	19.93	-155.10	50	6.0
November 29, 1975	19.36	-155.05	8	6.0
June 26, 1989	19.36	-155.08	9	5.8
October 15, 2006	19.88	-155.93	38	6.2

<sup>1</sup>Auxiliary materials are available in the HTML. doi:10.1029/2007GL031006.

**Table 2.** Discontinuity Depths and Impedance Contrasts

Discontinuity	z, km	R(z), %
<i>Synthetic 1</i>		
G	101	-5.5
410	435	2.3
520	513	1.2
660	662	5.5
<i>Synthetic 2</i>		
G	100	-5.5
L	224	1.2
X	288	1.1
410	435	2.3
520	511	1.1
660	663	5.6
Mid-Mantle	994	1.3

incidence  $T_{ScS}$  of 937.17 s at a frequency of 30 mHz. We scaled  $T_{ScS}$  to a frequency of 1 Hz for comparison to PREM ( $\delta T_{ScS} = +2$  s slow) [Dziewonski and Anderson, 1981] and IASP91 (+1.9 s slow) [Kennett and Engdahl, 1991]. We then adjusted the calculated time to match PREM and IASP91 crustal structures to remove a shallow component to the residual. The corrected  $\delta T_{ScS}$  we compute is 1.131 s fast for PREM, 0.425 s slow for IASP91, and consistent with zero in both cases.

#### 4. Discussion

[11] The resulting TZT is 227 km, which is thinner than the global average of 241–242 km [Flanagan and Shearer, 1998; Lawrence and Shearer, 2006]. The thinned TZ we infer is created primarily through the depression of the 410-km discontinuity to a path-averaged depth of 435 km. If this depression is of purely thermal origin, the deflection relative to the global mean depth of 418 km [Flanagan and Shearer, 1998] corresponds to a temperature increase of 129 K [Katsura et al., 2004]. We observe the 660-km discontinuity at 662 km depth, within error (5–7 km) [Revenaugh and Jordan, 1989] of the global mean value of 660 km [Flanagan and Shearer, 1998]. The temperature anomaly inferred to produce the 410-km depression should also cause the 660-km discontinuity to shallow by 1.7–8.5 km due to the negative Clapeyron slope of the post-spinel transformation at 660 km [Katsura et al., 2003]. Though we do not observe the expected shallowing at 660 km, the lower bound of the deflection predicted by the Clapeyron slope is within error of our measurement. Additionally, the post-garnet transition in this region of the mantle may counteract the expected shallowing of the 660-km discontinuity [Hirose et al., 2001] and so our observation is consistent with a hot thermal anomaly extending through at least TZ depths.

[12] The TZT can also be related to a temperature perturbation using constraints from phase relations and seismic velocities [Stixrude and Lithgow-Bertelloni, 2005]. This method is less biased by the velocity and tomography models used in the depth calculations, yielding a likely more accurate estimate of the thermal anomaly, although multiple phase transitions at the base of the TZ may bias the result. The 227 km TZT corresponds to a temperature increase of 87 K. The temperature calculation based on TZT [Stixrude and Lithgow-Bertelloni, 2005] considers the

influence of a peridotite phase assemblage rather than basing the temperature on the olivine component alone; this partly accounts for the differences in temperature calculated with the two methods. The thermal anomalies calculated from both the TZT and discontinuity depth deviations are consistent with the increase of 50–250 K observed from petrologic thermometers at ocean island basalts relative to mid-ocean ridge basalts [Lee et al., 2006], indicating that the temperature anomaly extends to at least TZ depths.

[13] The deviation of  $T_{ScS}$  from the reference models is smaller than expected based on most tomographic velocity maps of the area (e.g., a delay of 2.7 s is expected based on tomography from Megnin and Romanowicz [2000]), but one must be careful to consider the particulars of the study area and other influences on  $T_{ScS}$ . Our results average  $T_{ScS}$  over an epicentral distance of  $3^\circ$ , which may damp out an anomalous travel time as multiple ScS reverberations travel away from the source, near the plume head, to the receiver. The proposed plume source at the base of the mantle is even farther to the southeast [Steinberger and O'Connell, 1998], which may amplify this effect. If the velocity structure is caused by a plume with narrow cross-sectional area [e.g., Sleep, 1990], the ScS phases may deviate from the expected path to take advantage of faster velocities outside the plume. These explanations likely contribute to some extent to our observation, but are unlikely able to completely cancel out the expected anomaly based on tomography.

[14] Other interpretations involve the plume structure in the lower mantle. One explanation is simply that the Hawaiian plume originates at the boundary between the upper and lower mantle rather than at the core-mantle boundary. This may reconcile the discrepancy in travel time

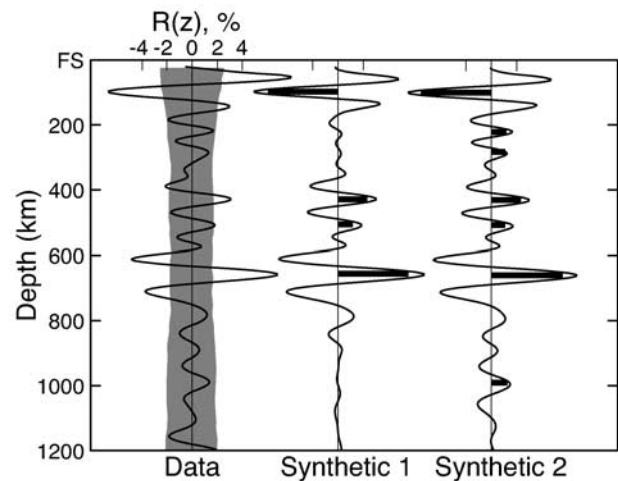


**Figure 2.** Reflectivity profile for the mantle beneath the study area for (left) data and (center and right) two synthetics. See text for description of synthetic profiles. Vertical axis is depth (km) from the free surface (FS); horizontal axis is reflection coefficient ( $R(z)$ , %). Tick marks on either side of center vertical line indicate  $R(z)$  of  $\pm 2\%$ . Peaks in the data profile exceeding the gray shaded region are significant at the 95% confidence level. Bold spikes show the amplitudes and depths of reflectors included in the synthetic models.

anomalies but is inconsistent with seismic observations of slow velocities beneath the TZ in the region. A similar explanation incorporates a whole-mantle plume with a lower-mantle structure that deviates away from the Hawaiian Islands. P-wave tomography [Montelli *et al.*, 2004] shows the plume branching into two structures located on either side of the Hawaiian Islands below approximately 1000 km depth. Our data may be sampling a thermal anomaly related to the plume in the upper mantle but sampling the area between plume branches in the lower mantle. S-wave tomography [Montelli *et al.*, 2006] shows similar structure for the mantle plume in the lowermost mantle, although in this model the anomalous thermal structure disappears in the lowermost mantle rather than branching into different areas.

[15] In the former scenarios, the  $T_{ScS}$  anomaly would be damped but likely still present to some extent, but there remain other considerations. Russell *et al.* [1999] observed anisotropy from  $ScS$  splitting above the core-mantle boundary beneath the Central Pacific near the Hawaiian plume. They proposed a horizontally sheared region with  $V_{SH}$  faster than  $V_{SV}$  ( $V_{SH} > V_{SV}$ ) extending laterally away from the plume source transitioning to  $V_{SH} < V_{SV}$  within the root and conduit of the mantle plume. The region of horizontal shear sampled by Russell *et al.* [1999] is approximately perpendicular in outline to our study area and is located to the southeast of the Hawaiian Islands. If we invoke radial symmetry of the plume structure such that this anisotropy extends outward from the plume in all directions, then our data would sample an anisotropic region near the core-mantle boundary with  $V_{SH} > V_{SV}$ . Similar anisotropy may be sampled near the surface as well, if there is preferred orientation of minerals aligned with plate motion of the Pacific Plate. Since our data is sensitive to  $V_{SH}$ , both of these anisotropic scenarios would reduce  $T_{ScS}$ , reducing any delay caused by a thermal plume structure. If this anisotropy is strong enough to neutralize  $T_{ScS}$  delays, then any azimuthal anisotropy beneath the study area should be strong enough to produce split  $ScS_n$  arrivals, especially when  $n > 1$ . We examine this by looking at particle motion plots for the  $ScS_2$  phase for each of the three events that provided suitable seismograms on both the radial and transverse components (Figure S3). We choose this phase for its balance of signal strength, which decreases with core-bounce number, and sensitivity to anisotropy, which increases with core bounces. All three  $ScS_2$  phases show ellipticity in the particle motion indicating a time difference of  $\sim 1$  s between the radial and transverse components of  $ScS$ , consistent with the interpretation of anisotropy at the base of the mantle. The 1 s delay does not greatly affect the  $ScS$  reverberations (frequency of  $\sim 30$  mHz), and our use of both the radial and transverse components in the analysis results in an “isotropic”  $T_{ScS}$  that is not biased toward fast or slow arrivals resulting from the anisotropy. A component of the elliptical particle motion may be produced by  $ScS_2$  waveform distortion due to an out-of-plane reflection from an inclined surface near the top or bottom of the mantle. Given the short epicentral distances involved, however, any such component must be small.

[16] An additional reduction in  $T_{ScS}$  could be produced by an ultra-low velocity zone (ULVZ) at the base of the mantle beneath the study area [e.g., Mori and Helmberger, 1995;

Revenaugh and Meyer, 1997; Russell *et al.*, 2001; Thorne and Garnero, 2004]. The  $ScS$  reverberations follow near-vertical raypaths and spend very little time in the ULVZ ( $< 4$  s), so slow velocities within these regions don't greatly affect  $T_{ScS}$ .  $ScS_n$ -precursors caused by reflections off of the top of a ULVZ, however, arrive shortly before  $ScS_n$  and are in phase, whereas the first (and strongest) reverberations within the layer arrive an equal time after  $ScS_n$  and are inverted. The effect of these  $ScS_n$ -pre- and post-cursors is to produce a distorted pulse that appears advanced in the scheme of the hierarchical waveform inversion/migration method.

## 5. Conclusions

[17] Mantle discontinuity depth observations indicate that the mantle beneath Hawaii is anomalously hot relative to ambient mantle conditions ( $\Delta T = 87\text{--}129$  K), suggesting that a thermal mantle plume originating from at least TZ depths feeds the Hawaiian hotspot. The vertical-incidence  $T_{ScS}$  measured beneath the area does not show the delay relative to reference mantle velocity models expected for an  $ScS$  phase traveling within a thermal plume originating from either the TZ or the core-mantle boundary. A portion of the discrepancy between the discontinuity and travel time observations may be a result of damping anomalous structure by averaging the mantle travel time over an epicentral distance of  $3^\circ$ , and by the fact that the location of the proposed plume is southeast of the study area rather than directly beneath it. The additional apparent discrepancy may be reconciled if the phases sample  $V_{SH} > V_{SV}$  anisotropy above the core-mantle boundary and if  $ScS$ -precursors caused by reflections from the top of a ULVZ at the base of the mantle affect the  $ScS$  waveforms. We interpret these observations as resultant effects of an inclined, and potentially branching, thermal plume originating at the core-mantle boundary, anisotropy caused by horizontal flow from surrounding areas into the plume conduit, and the  $ScS$  waveform bias towards earlier travel times related to ULVZ structure at the base of the mantle.

[18] **Acknowledgments.** This research was funded by the National Science Foundation (EAR-0437424) and a University of Minnesota Doctoral Dissertation Fellowship (AMC).

## References

- Allen, R. M., et al. (1999), The thin hot plume beneath Iceland, *Geophys. J. Int.*, *137*, 51–63.
- Anderson, D. L. (2000), The thermal state of the upper mantle: No role for mantle plumes, *Geophys. Res. Lett.*, *27*, 3623–3626.
- Anderson, D. L. (2005), Scoring hotspots: The plume and plate paradigms, in *Plates, Plumes, and Paradigms*, edited by G. R. Foulger et al., *Spec. Pap. Geol. Soc. Am.*, *388*, 31–54.
- Deuss, A., and J. H. Woodhouse (2002), A systematic search for mantle discontinuities using SS-precursors, *Geophys. Res. Lett.*, *29*(8), 1249, doi:10.1029/2002GL014768.
- Dziewonski, A. M., and D. L. Anderson (1981), Preliminary reference Earth model, *Phys. Earth Planet. Inter.*, *25*, 297–356.
- Flanagan, M. P., and P. M. Shearer (1998), Global mapping of topography on transition zone velocity discontinuities by stacking SS precursors, *J. Geophys. Res.*, *103*, 2673–2692.
- Helffrich, G. (2000), Topography of the transition zone seismic discontinuities, *Rev. Geophys.*, *38*, 141–158.
- Herzberg, C. (2006), Petrology and thermal structure of the Hawaiian plume from Mauna Kea volcano, *Nature*, *444*, 605–609.
- Hirose, K., Y. Fei, S. Ono, T. Yagi, and K.-I. Funakoshi (2001), In situ measurements of the phase transition boundary in  $Mg_3Al_2Si_3O_{12}$ : Impli-

- cations for the nature of the seismic discontinuities in the Earth's mantle, *Earth Planet. Sci. Lett.*, *184*, 567–573.
- Katsura, T., et al. (2003), Post-spinel transition in  $Mg_2SiO_4$  determined by high P-T in situ x-ray diffractometry, *Phys. Earth Planet. Inter.*, *136*, 11–24.
- Katsura, T., et al. (2004), Olivine-wadsleyite transition in the system  $(Mg, Fe)_2SiO_4$ , *J. Geophys. Res.*, *109*, B02209, doi:10.1029/2003JB002438.
- Kennett, B. L. N., and E. R. Engdahl (1991), Travel times for global earthquake location and phase identification, *Geophys. J. Int.*, *105*, 429–465.
- Lawrence, J. F., and P. M. Shearer (2006), A global study of transition zone thickness using receiver functions, *J. Geophys. Res.*, *111*, B06307, doi:10.1029/2005JB003973.
- Lay, T., and T. C. Wallace (1983), Multiple ScS travel times and attenuation beneath Mexico and Central America, *Geophys. Res. Lett.*, *10*, 301–304.
- Lee, C.-T. A., A. Courtier, R. Halama, M. Jackson, A. Larson, J. Lawrence, Z. Wang, J. Warren, R. Workman, W. Xu, M. Hirschmann, S. Hart, L. Stixrude, C. Lithgow-Bertelloni, and W.-P. Chen (2006), The thermal state of the Earth, *Eos Trans. AGU*, *87*(52), Fall Meet. Suppl., Abstract V33D-08.
- Lei, J., and D. Zhao (2006), A new insight into the Hawaiian plume, *Earth Planet. Sci. Lett.*, *241*, 438–453.
- Li, X., R. Kind, K. Priestley, S. V. Sobolev, F. Tilmann, X. Yuan, and M. Weber (2000), Mapping the Hawaiian plume with converted seismic waves, *Nature*, *405*, 938–941.
- Megnín, C., and B. Romanowicz (2000), The three-dimensional shear velocity structure of the mantle from the inversion of body, surface and higher-mode waveforms, *Geophys. J. Int.*, *143*, 709–728.
- Montelli, R., G. Nolet, F. A. Dahlen, G. Masters, E. R. Engdahl, and S.-H. Hung (2004), Finite-frequency tomography reveals a variety of plumes in the mantle, *Science*, *303*, 338–343.
- Montelli, R., G. Nolet, F. A. Dahlen, and G. Masters (2006), A catalogue of deep mantle plumes: New results from finite-frequency tomography, *Geochem. Geophys. Geosyst.*, *7*, Q11007, doi:10.1029/2006GC001248.
- Mori, J., and D. V. Helmberger (1995), Localized boundary layer below the mid-Pacific velocity anomaly identified from a PcP precursor, *J. Geophys. Res.*, *100*, 20,359–20,365.
- Okal, E., and D. L. Anderson (1975), A study of lateral inhomogeneities in the upper mantle by multiple ScS travel time residuals, *Geophys. Res. Lett.*, *2*, 313–316.
- Revenaugh, J., and T. H. Jordan (1989), A study of mantle layering beneath the western Pacific, *J. Geophys. Res.*, *94*, 5787–5813.
- Revenaugh, J., and T. H. Jordan (1991a), Mantle layering from ScS reverberations: 1. Waveform inversion of zeroth-order reverberations, *J. Geophys. Res.*, *96*, 19,749–19,762.
- Revenaugh, J., and T. H. Jordan (1991b), Mantle layering from ScS reverberations: 2. The transition zone, *J. Geophys. Res.*, *96*, 19,763–19,780.
- Revenaugh, J., and R. Meyer (1997), Seismic evidence of partial melt within a possibly ubiquitous low-velocity layer at the base of the mantle, *Science*, *277*, 670–673.
- Russell, S. A., T. Lay, and E. J. Garnero (1999), Small-scale lateral shear velocity and anisotropy heterogeneity near the core-mantle boundary beneath the central Pacific imaged using broadband ScS waves, *J. Geophys. Res.*, *104*, 13,183–13,199.
- Russell, S. A., C. Reasoner, T. Lay, and J. Revenaugh (2001), Coexisting shear- and compressional-wave seismic velocity discontinuities beneath the central Pacific, *Geophys. Res. Lett.*, *28*, 2281–2284.
- Schmer, N., and E. Garnero (2006), Investigation of upper mantle discontinuity structure beneath the central Pacific using SS precursors, *J. Geophys. Res.*, *111*, B08305, doi:10.1029/2005JB004197.
- Shen, Y., C. J. Wolfe, and S. C. Solomon (2003), Seismological evidence for a mid-mantle discontinuity beneath Hawaii and Iceland, *Earth Planet. Sci. Lett.*, *214*, 143–151.
- Sipkin, S. A., and T. H. Jordan (1980), Regional variation of QScS, *Bull. Seismol. Soc. Am.*, *70*, 1071–1102.
- Sleep, N. H. (1990), Hotspots and mantle plumes: Some phenomenology, *J. Geophys. Res.*, *95*, 6715–6736.
- Sleep, N. H. (2006), Mantle plumes from top to bottom, *Earth Sci. Rev.*, *77*, 231–271.
- Steinberger, B., and R. J. O'Connell (1998), Advection of plumes in mantle flow: Implications for hotspot motion, mantle viscosity and plume distribution, *Geophys. J. Int.*, *132*, 412–434.
- Stixrude, L., and C. Lithgow-Bertelloni (2005), Thermodynamics of mantle minerals - I. Physical properties, *Geophys. J. Int.*, *162*, 610–632.
- Takahashi, E., K. Nakajima, and T. L. Wright (1998), Origin of the Columbia River basalts: Melting model of a heterogeneous plume head, *Earth Planet. Sci. Lett.*, *162*, 63–80.
- Thorne, M. S., and E. J. Garnero (2004), Inference on ultralow-velocity zone structure from a global analysis of SpdKKS waves, *J. Geophys. Res.*, *109*, B08301, doi:10.1029/2004JB003010.
- Vinnik, L., M. Ravi Kumar, R. Kind, and V. Farra (2003), Super-deep low-velocity layer beneath the Arabian plate, *Geophys. Res. Lett.*, *30*(7), 1415, doi:10.1029/2002GL016590.
- Woodhouse, J. H., and A. M. Dziewonski (1984), Mapping the upper mantle: Three dimensional modeling of Earth structure by inversion of seismic waveforms, *J. Geophys. Res.*, *89*, 5953–5986.

---

B. Bagley, A. M. Courtier, and J. Revenaugh, Department of Geology and Geophysics, University of Minnesota, 310 Pillsbury Drive SE, Minneapolis, MN 55455, USA. (bagl0025@umn.edu; cour0090@umn.edu; justinr@umn.edu)